

Micromanipulation system for insect sensilla based on shape memory $Ti_{50}Ni_{25}Cu_{25}$ alloy

© S.V. von Gratowski,¹ M.I. Zhukovskaya,² A.M. Lunichkin,² A.V. Shelyakov,³ N.N. Sitnikov,⁴ V.V. Koledov,^{1,5} K.A. Borodako,^{1,3} S.F. Petrenko⁵

¹ Kotelnikov Institute of Radioengineering and Electronics (IRE) of Russian Academy of Sciences, Moscow, Russia

² Sechenov Institute of Evolutionary Physiology and Biochemistry, Russian Academy of Sciences, Saint-Petersburg, Russia

³ National Research Nuclear University MEPhI (Moscow Engineering Physics Institute), Moscow, Russia

⁴ State Scientific Center of the Russian Federation „Keldysh Research Center“, Moscow, Russia

⁵ Sirius University of Science and Technology, Sochi, Russia

e-mail: svetlana.gratowski@yandex.ru

Received March 4, 2023

Revised May 16, 2023

Accepted May 25, 2023

Insect pest control requires fundamental knowledge of their physiology and behavioral responses. However, due to the small size of insects, in general, and their sensory organs (sensilla), in particular, the study of the physiology of insect sensory systems has until recently been limited by insufficient accuracy and selectivity of experimental mechanical manipulation. To eliminate this gap in the study of insects, a physical technology is proposed based on a micromechanical device - microtweezers based on a layered structural composite of $Ti_{50}Ni_{25}Cu_{25}$ alloy with a shape memory effect (SME), combined with a temperature control system and a three-coordinate piezoelectric micropositioner. Microtweezers with SME selectively capture the smallest sensilla of the studied insects, enabling their precise mechanical stimulation with simultaneous recording of physiological responses generated by sensilla using methods of impulse derivation in the nerve centers of the insect.

Keywords: shape memory alloys, shape memory effect (SME), microtweezers, insect sensilla, impulse conduction in insect nerve centers.

DOI: 10.61011/TP.2023.08.57277.37-23

Introduction

Due to their abundance and diversity, insects play an extremely important role in agroecosystems (places where agriculture is carried out). Pest insects cause enormous damage to both crops and food stocks in warehouses. On the other hand, chemical means of combating them have many negative effects on pollinators and entomophages. Consequently, the search for fundamentally new approaches to the problem of controlling the behavior of insects is of great importance. In this regard, the experimental study of the nervous activity of insects and, in particular, their sensory system is of decisive importance. The sensory apparatus and the set of attractive, repellent and aversive mechanical and chemical stimuli perceived by insects are quite species-specific. Therefore, an experimental study of the sensory organs of various insects is absolutely necessary in order to evaluate, and then carry out modeling and testing in the laboratory and field conditions of the most effective stimuli and their combinations, in principle, allowing to influence on the behavior of insects.

Insects are an inexhaustible source of microminiature technical solutions created over millions of years of biological evolution. Sensory physiology of insects is a rapidly developing field of science. The operating principles of their miniature receptor structures are used in the design of materials with unusual properties, micromechanical devices

and sensors [1,2]. During evolution, the need for orientation in space, avoidance of danger, search for food and sexual partners led to the occurrence of a variety of sensory structures, most of which are built on a similar principle and have a common origin.

Insect sensilla are derivatives of a hollow cuticular hair with sensory cells inside, which perceive mainly mechanical and chemical stimuli. Modified mechanoreceptor sensilla can respond to infrared radiation, changes in humidity [3,4], and also serve as proprioceptors, signaling the relative position of body parts [5,6]. The evolutionarily basic type of sensilla found in most modern insects is — trichoid (hair-like) sensilla — these are hollow chitinous tubes with a diameter from fractions of a micron to tens of microns. The length of the sensilla varies from $8\mu\text{m}$ in insects such as *Megaphragma mymaripenne* with a body length of $235\mu\text{m}$ only [7] and the american cockroach *Periplaneta americana*, up to 5 cm [8] long, up to $2200\mu\text{m}$ for the cave cricket *Phaeophilacris bredoides*, whose body length is about 2 cm [9].

Sensory neurons within the sensilla respond to adequate stimulation by increasing the frequency of spikes (electrical impulses), which can be recorded extracellularly using a microelectrode, while the small number of sensory neurons in the sensilla allows spikes from each cell to be distinguished by their size and shape [10]. The largest number of sensilla in crickets and related insects are located

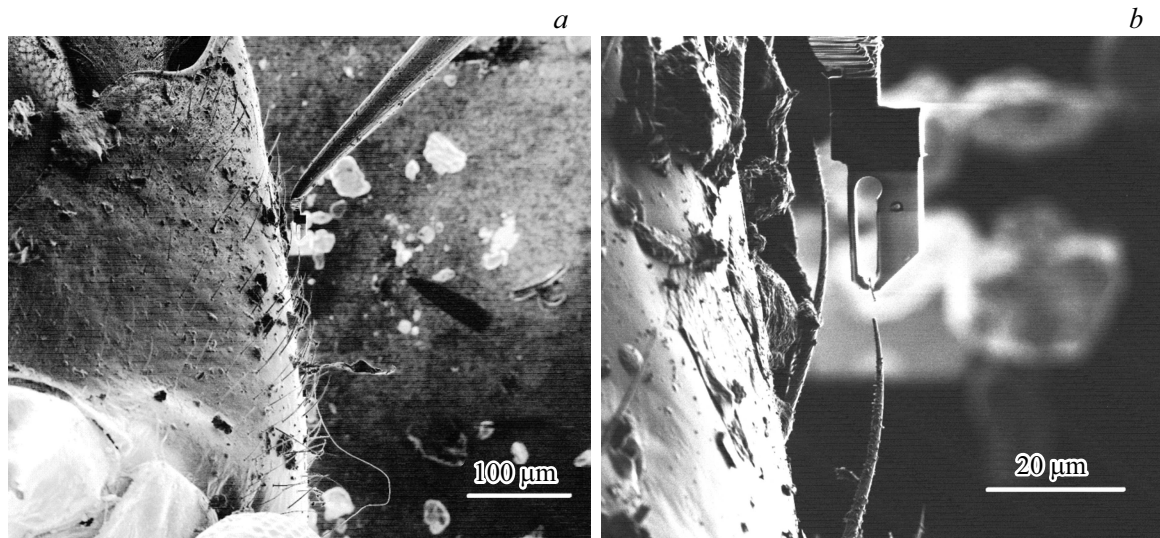


Figure 1. *a* — selection of an individual sensilla of a mosquito *C. pipiens* using nanotweezers with SME mounted on a tungsten microneedle, which is positioned by Omniprobe nanomanipulator in the vacuum chamber of FEI Strata 201 FIB ion microscope (measuring ruler 100 μm). *b* — capture and cutting of a fragment of the *C. pipiens* sensilla with an ion beam of FEI Strata 201 FIB microscope (measuring ruler 20 μm).

on two pairs of sensory organs — antennae located on the head, and cerci — paired appendages of the abdomen, but some of the sensilla are located on the limbs, wings and surface of the body. A detailed study of the behavioral responses of crickets that do not sing and have no tympanal (auditory) organs indicates the ability of these insects to perceive sounds. Low-frequency sounds cause vibrations of the filiform sensilla, which are maximum when the resonant frequency of the natural vibrations of the hair and the sound acting on it coincide and, accordingly, cause the greatest behavioral response [11].

The morphological features of mechanosensory and chemomechanosensory (gustatory) sensilla indicate the inequality of different directions of hair deflection, however, direct experimental studies in this area are limited by the coarseness of the tools used, such as air flow [12]. The base of the sensilla is connected to the main cuticle of the antenna by a soft and elastic articular membrane, which contains a lot of resilin protein, which ensures special properties [2]. The morphologically complex arrangement of articulation of wind-sensitive sensilla plays a significant role in the movements of the section with which the receptor cell is in contact [13].

Mechanosensitive sensilla hairs of different lengths have oscillation resonant frequencies from 0.01 to 1 kHz [14,15]. Modeling of hair oscillations under the influence of air flows using the Euler–Bernoulli equation revealed additional oscillation resonant frequencies, and the next frequency after the main one is approximately by 6 times higher, and the oscillation amplitude is by an order of magnitude smaller [16]. Behavioral responses of crickets to sound confirm the appearance of an additional peak in the sensitivity of the cercal organ at frequencies approximately

by 6 times higher than the main one with an amplitude by order of magnitude smaller. In our case, responses to sounds 3–6 kHz are given by the same sensilla that are sensitive to sound 0.5–1 kHz of lower intensity [9].

The responses of the mechanoreceptor neuron in the contact chemomechanosensory sensilla are shown [17], but practically are not studied, since, on the one hand, the responses of chemosensory cells are of greatest interest, and on the other hand the widely used method of tip recording does not allow us to isolate rapidly adapting responses of the mechanosensory neuron due to artifacts when the recording electrode contacts the sensilla, as well as to change the position of the sensilla hair with precisely controlled parameters — deflection and its speed.

Stimulation by air flows and acoustic vibrations complicates electrophysiological recordings, creating artifacts. Stimulation of the mechanoreceptor of the contact chemomechanosensory sensilla in the paper of Marion–Poll [17] was performed by moving the recording electrode, which did not allow evaluation of the stimulus-response relationship and obtaining reproducible data on the impulse activity of the mechanosensory neuron. Despite significant success, the sensory physiology of insects requires the use of new methods and tools for qualitative progress in understanding the mechanisms of mechanoreception, especially at the level of perireceptor events, namely the primary transformation of stimulus energy into the receptor potential of the sensory cell.

Modern nanotechnology has unique methods that allow manipulation, i.e. selection, capture, movement in three-dimensional space of individual micro- and nanoobjects, such as nanotubes, nanowires, etc. [18–21]. Previously attempts were made to manipulate insect sensilla using

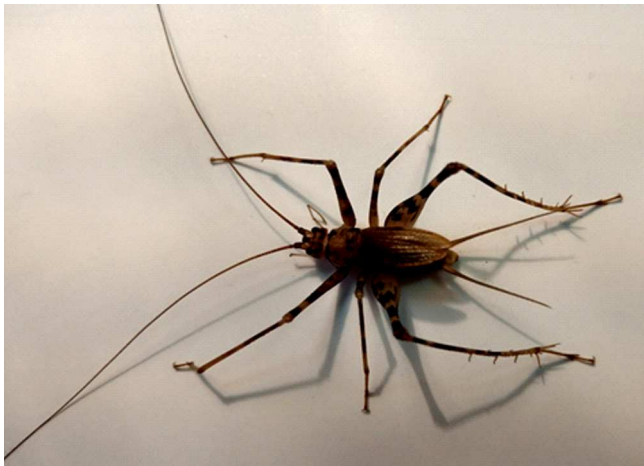


Figure 2. Adult male cricket *Phaeophilacris bredoides*.

nanopositioners and shape memory effect (SME) nanotweezers in the vacuum chamber of a scanning ion microscope [22]. Fig. 1 shows micrographs obtained in the scanning ion microscope, reflecting the process of capturing and manipulating the sensilla of mosquito *Culex pipiens* using composite nanotweezers with an SME mounted on Omniprobe micromanipulator. In these experiments, the control of the nanotweezers, its closing and opening, is carried out by local heating of the nanotweezers using the radiation of a semiconductor injection laser built into FEI Strata 201 FIB ion microscope. The tip of the sensilla (Fig. 1, *b*) is cut off by the ion beam of the ion microscope in its vacuum chamber. However, experimental work to study the sensory mechanism of insects *in vivo* requires

a comprehensive solution to the problem of observing the entire sensory organ of the insect, for example, the cerci, in natural conditions, selecting and controlled mechanical stimulation of one of the many individual sensilla, as well as microelectrode recordings of nerve impulses, caused by this stimulation.

The goal of this paper is to develop a method for studying the neural response of individual insect mechanosensitive sensilla. This method is distinguished by accuracy and selectivity due to the use of micromechanical devices: microtweezers made of a composite based on an alloy of the quasi-binary system TiNi – TiCu with SME, combined with a three-dimensional nanopositioner based on piezomotors.

1. Experiment procedure

Adult male cave crickets *Ph. bredoides*, whose appearance is shown in Fig. 2, were chosen as the object of the study. According to data of scanning electron microscopy, the cerci are covered with a large number of sensory structures, sensilla, which can be divided into four types: club-shaped, setaceous, filiform (Fig. 3, *a*) and campaniform (Fig. 3, *b*).

Club-shaped sensilla are located only at the base of the cerci and are involved in the perception of gravity force [23]. Campaniform sensilla, located near the base of filiform sensilla, presumably expand the dynamic range of signals, causing qualitatively different behavioral responses to strong stimuli [24].

Since chemomechanoreceptor (taste) sensilla are characterized by a pore at the tip through which chemicals penetrate to the receptor cell, cercal sensilla were studied using iontophoretic staining. To do this, the end of the

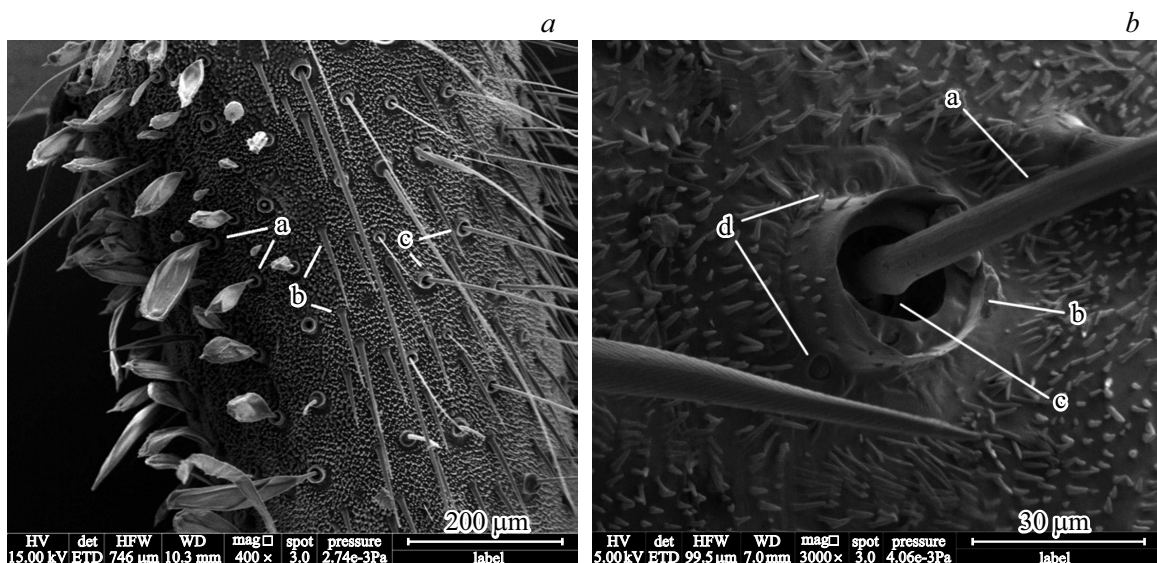


Figure 3. SEM image of the cerci of cricket *Ph. bredoides*: *a* — general view of the cercus surface, *a* — club-shaped sensilla, *b* — bristle-shaped sensilla, *c* — filiform sensilla; *b* — campaniform sensilla at the base of filiform sensilla on the cercus of *Ph. bredoides*. *a* — hair of wind-sensitive sensilla, *b* — cuticular cup, *c* — articulated membrane, *d* — campaniform sensilla.

cricket's abdomen with the cerci was placed in a cuvette with a 0.05% cobalt chloride solution, and a silver chloride electrode was connected to the solution. The second electrode of the same type was in contact with the cricket's abdomen through a micropipette filled with saline. A direct current of 1 mA was passed through the preparation for 30 min. Then the cerci were cut off, incubated in a 2% ammonium sulfide solution for 12 h to precipitate cobalt, and then viewed under a Micromed MS1 binocular microscope and images were photographed using DCM-130E SCOPE video camera.

To study the parameters of mechanoreceptive responses of filiform and bristle-like sensilla, a special micromanipulation system was developed and manufactured, including a micromechanical tool (micropweezers) with a control unit (device) and a three-coordinate positioner. The system allows you to capture the individual sensilla and deflect it in a predetermined manner.

2. Results and discussion

Preliminary morphological studies indicate the predominance of two types of sensilla (Fig. 4): filiform, at the base of which there is a ring-shaped cuticular cup, and bristle-shaped, with a simple cuticular thickening in the basal part. The bristle-shaped sensilla turned out to be intensely stained, indicating the presence of a pore through which the dye enters. Functionally, these sensilla can be classified as mechano-chemoreceptor. The filiform sensilla remained unstained, which confirms their sensitivity to mechanical stimuli only.

In this study, the alloy $\text{Ti}_{50}\text{Ni}_{25}\text{Cu}_{25}$, obtained by rapid melt quenching in the form of a thin ribbon, was selected for the development of microtweezers. It is well known that rapidly quenched alloys of the quasi-binary system TiNi-TiCu with a copper content of more than 17 at.%

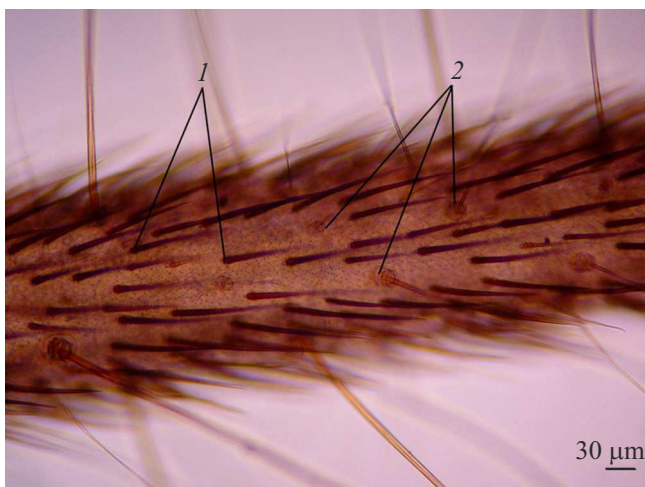


Figure 4. Cricket cercus *Ph. bredoides* iontophoretic staining with cobalt chloride. 1 — stained contact chemoreceptor sensilla; 2 — unstained mechanoreceptor filiform sensilla.

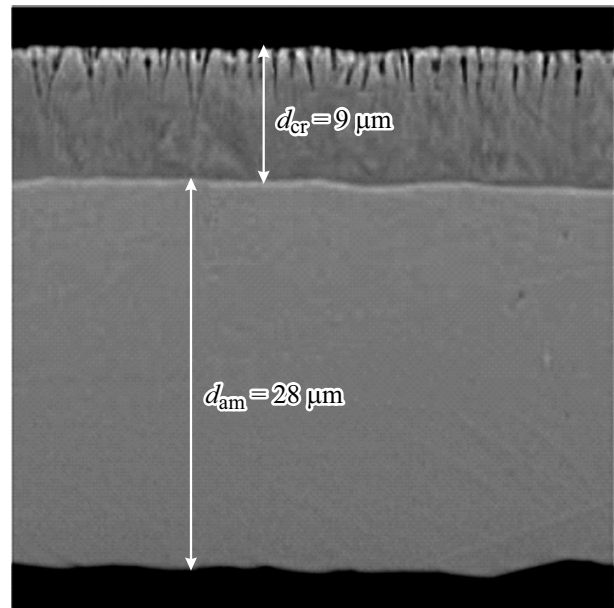


Figure 5. Representative electron microscopic image of the cross section of the amorphous-crystalline ribbon of alloy $\text{Ti}_{50}\text{Ni}_{25}\text{Cu}_{25}$.

have a high tendency to amorphization and acquire a pronounced SME after special heat treatment [25]. It was previously shown that in this alloy, at melt cooling rates in the range $10^5 - 10^6$ K/s, a layered amorphous-crystalline structural composite with a sharp interface [26] is formed. In this paper, a series of samples of rapidly quenched composite ribbons was manufactured, in them the ratio of the thicknesses of the amorphous and crystalline layers varied by changing the cooling rate of the melt. The electron microscopic image of the characteristic cross section of the amorphous-crystalline ribbon is shown in Fig. 5. Samples were obtained with thicknesses of the crystalline d_{cr} and amorphous d_{am} layers in the range from 5.40 to 9.80 μm and from 35.01 to 24.09 μm accordingly.

The resulting samples of layered amorphous-crystalline composites after quenching exhibit a two-way SME (TWSME) with bending deformation. The effect implementation is illustrated in Fig. 6: in the initial state at room temperature (below the temperature of the end of the martensitic transformation M_f in the crystalline layer) the ribbon has a shape close to rectilinear; after heating above the temperature of the end of the austenitic transformation A_f , the sample takes a shape close to a ring, and when cooled to room temperature it returns to its original rectilinear shape. Paper [26] describes a model for the TWSME occurrence in layered amorphous-crystalline structure, according to which the crystalline layer becomes stretched after the quenching process, and, when heated above the temperature A_f it tends to compress due to the SME implementation, which leads to bending of the composite. When cooled, due to the elasticity of the amorphous layer, the composite returns to its original state. It was experimentally established that when the temperature

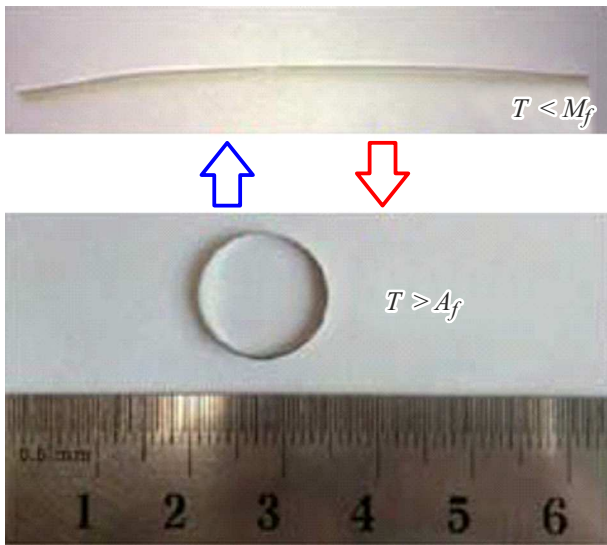


Figure 6. Implementation of the TWSME in amorphous-crystalline composite made of rapidly quenched alloy $Ti_{50}Ni_{25}Cu_{25}$.

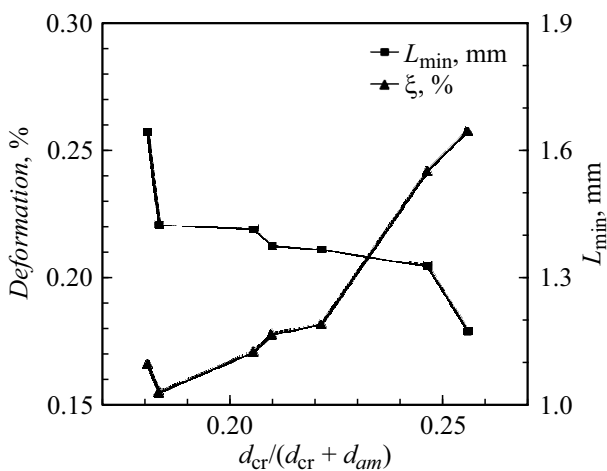


Figure 7. Deformation ε and minimum length of ribbon L_{min} , which ensures movement of the free end $\Delta = 60 \mu m$ vs. thickness ratio $d_{cr}/(d_{cr} + d_{am})$.

changes in the martensitic transformation range, a reversible change in the shape of the composite can be repeated cyclically more than 20 000 times.

The minimum bending radius R_{min} was measured for TWSME manifestation in samples prepared at different cooling rates. The reversible bending deformation during the TWSME manifestation was calculated: $\varepsilon = (d_{cr} + d_{am})/(2R_{min})$. ε vs. thicknesses ratio of amorphous and crystalline layers is shown in Fig. 7.

The conducted studies of amorphous-crystalline ribbons made it possible to preliminary estimate the geometric parameters of microtweezers based on them. In particular, to capture micro-objects with a characteristic size of up to $100 \mu m$, the acceptable initial value of the microgrip gap shall be approximately $120 \mu m$. If the microgrip

consists of two ribbons connected to each other with the ability to bend towards each other due to the TWSME, to ensure complete closure when heated the movement of the free end of the ribbon shall be at least $60 \mu m$. For the ribbon L long, one end of which is rigidly fixed, and the other end, when heated, is displaced by Δ , the following relation was obtained from geometric calculations: $L = 2 \cdot R_{min} \cdot \arccos(\Delta/R_{min})$. The minimum length of the working part of microtweezers L_{min} , it ensures movement of the free end $\Delta = 60 \mu m$, was calculated depending on the ratio $d_{cr}/(d_{cr} + d_{am})$ (Fig. 7).

When choosing the ribbon, its homogeneity through thickness and surface roughness were taken into account. On the contact side of the tape, surface defects are formed due to the quality of polishing of the quenching wheel, as well as the possible influence of the unsteadiness of the melt jet, for example, the possible gas entry into the area between the melt and the wheel or the initiation of vortices in the moving melt. The non-contact (free) side of the ribbon has a relatively lower roughness, but its thickness noticeably decreases from the center of the ribbon to the edges. Experimental measurements on a profilometer showed that for the contact surface of the ribbons the average deviation R_a is in the range from 0.63 to $0.85 \mu m$, the standard deviation $R_q = 0.87 - 1.05 \mu m$, at the same time for the non-contact surface $R_a = 1.25 - 1.75 \mu m$, $R_q = 1.35 - 1.62 \mu m$.

As a result of the studies, for the microtweezers manufacturing a sample with $d_{am} = 24.69 \mu m$, $d_{cr} = 7.03 \mu m$, $R_{min} = 8 \mu m$ ($\varepsilon = 0.182\%$), $L_{min} = 1.32 mm$, which has an optimal combination of mechanical (shape memory) and surface properties was selected. The temperatures of the beginning and end of this ribbon shape restoration upon heating were measured: $A_s = (48.2 \pm 0.5)^\circ C$ and $A_f = (57.1 \pm 0.5)^\circ C$ respectively.

The procedure for microtweezers manufacturing was as follows. Two pieces of ribbon were superimposed on each other with the ability to bend towards each other when heated. In this case, to set the initial gap of the microtweezers a spacer made of a completely amorphous ribbon of alloy $TiNiCu$ was placed between them, the ribbon does not exhibit SME when heating and cooling. Further, the ribbons were connected by microwelding, forming a three-layer sandwich (Fig. 8).

Microtweezers were installed in the temperature monitoring device based on Peltier element. The schematic view of the device is shown in Fig. 9. It includes a base 1 made of silver, on which microtweezers 2 are attached. The base is located on Peltier element 3, which heats or cools it. The thermistor 4 measures the temperature of the base 1. The Peltier element, the thermistor and the base are mounted on the console 5, which is attached to a connector 6 connected to three-axis positioner with a thin pin 7. The device is controlled by the DX5100 controller, which is a precision programmable control unit for thermoelectric coolers (Peltier elements). The controller implements bidirectional (heating and cooling) control and allows you to maintain the set temperature of the device

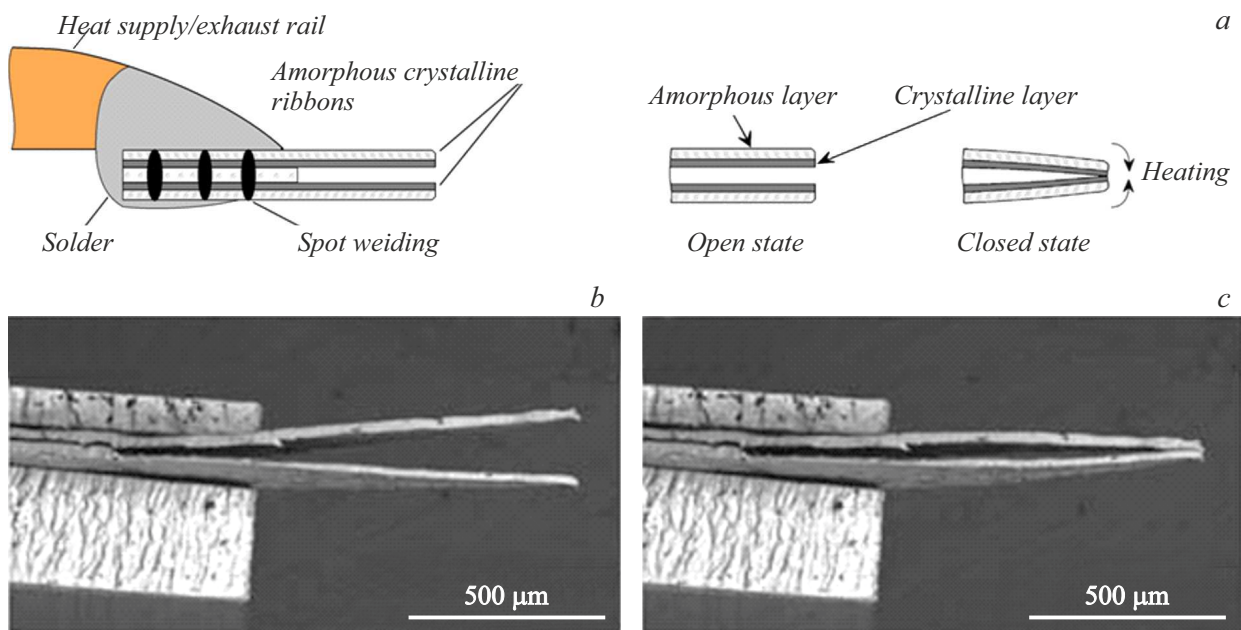


Figure 8. Schematic representation of microtweezers based on a composite ribbon with TWSME (a). SEM image of microtweezers in open (b) and closed (c) states.

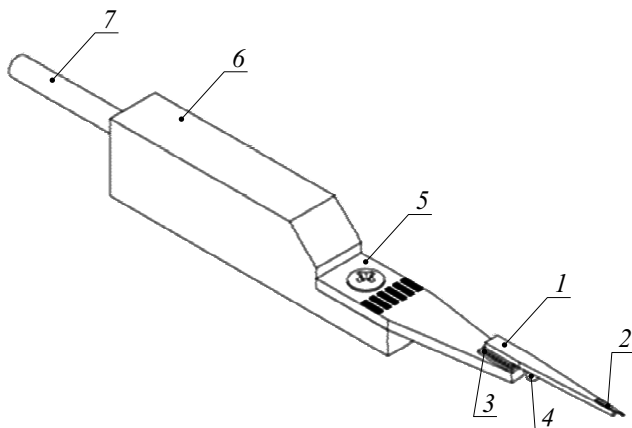


Figure 9. Diagram of temperature monitoring device for microtweezers control. Explanations in the text.

with high accuracy or carry out a specified heating and cooling program over time.

The temperature dependence of the response time (closing and opening) of the microtweezers was measured in the environment according to the method described in [20]. First of all in device the initial temperature T_1 is set below the beginning of the martensitic transformation in the alloy $\text{Ti}_{50}\text{Ni}_{25}\text{Cu}_{25}$, which in general may be either higher or lower than room temperature. Thus, at set temperature the alloy $\text{Ti}_{50}\text{Ni}_{25}\text{Cu}_{25}$ is reliably in the martensitic phase. Then preheating occurs to temperature T_2 , close to the temperature of the austenitic transformation beginning. Temperature increasing to temperature T_3 above the temperature of the end of the austenitic transformation leads to the microtweez-

ers closure. Cooling to the initial temperature T_1 causes the microtweezers opening. The device operating cycle can then be repeated, if necessary. The optimal operating mode of the microtweezers was selected: preheating temperature $T_2 = 45^\circ\text{C}$ and overheating temperature $T_3 = 71^\circ\text{C}$, the optimal times for closing and opening the tweezers were 1.1 and 1.7 s, respectively. It is important to note that under vacuum conditions the time characteristics of the microtweezers were the same as in the environment.

To move the microtweezers a three-coordinate positioner was used with a step $1\ \mu\text{m}$, and its operation was observed in the optical microscope. With the help of the developed system the complete technological process of manipulating the micro-object is implemented: capture–holdinh–movement–release. Fig. 10 demonstrates manipulation of the sensilla of the African cave cricket *Ph. bredoides*, which were selectively captured and deflected with a given amplitude.

Conclusion

The paper proposes a method for studying the mechanosensitive sensilla of insects, which consists of applying precision mechanical stimuli to the mechanoreceptor and chemomechanoreceptor (taste) sensilla of insects using micromanipulation system. The main results of the paper are as follows:

1. The method of melt ultra-rapid quenching produced series of layered amorphous-crystalline composites of the alloy $\text{Ti}_{50}\text{Ni}_{25}\text{Cu}_{25}$, possessing a two-way shape memory effect, with different ratio of thicknesses of the amorphous and crystalline layers.

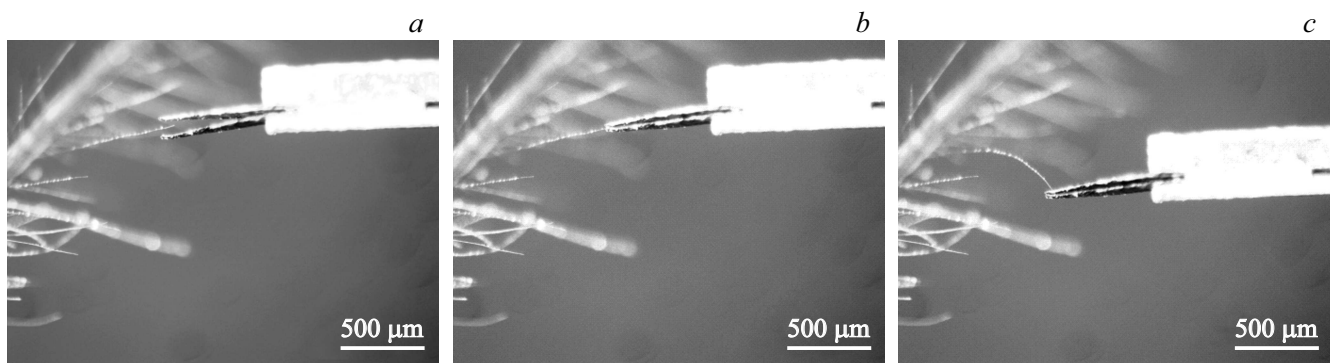


Figure 10. Manipulating the sensilla of cricket *Phaeophilacris bredoides* using microtweezers (*a* — microtweezers are brought to the filiform sensilla; *b* — grasping the tip of the sensilla; *c* — sensilla derivation).

2. The resulting functional composites served as the basis for the manufacture of series of microtweezers with adjustable gap in the range of 5 to 120 μm , the width of the gripping parts 400–500 μm and their characteristic length of 650 to 1300 μm depending on the gap size.

3. It was revealed that the time characteristics of microtweezers significantly depend on the control temperature regime. Optimal control parameters provide response times (closing and opening) of microtweezers of 1.1 and 1.7 s, respectively.

4. The possibility of manipulating — capturing and deflecting the cuticular part of the sensilla using the manipulation system based on rapidly quenched amorphous-crystalline ribbon made of alloy $\text{Ti}_{50}\text{Ni}_{25}\text{Cu}_{25}$ with two-way shape memory effect. In the future, using the proposed method and calculations of the mechanical properties of the hair cuticle and the articular structure, it will be possible to estimate both the dynamic range of deviations in which the sensilla function, as well as the exact relationships between the degree of hair deviation, the direction of this deviation, and the parameters of the electrical response of the receptor cell. The data obtained will be useful not only for analyzing the sensory system of insects, but also for designing miniature and reliable mechanical sensors.

Funding

The study of the physiological characteristics of the nervous system of insects was carried out within the framework of state assignment № 075-00967-23-00, work on the creation of a micromanipulation system was carried out under a grant with the financial support of grant from the Russian Science Foundation (project № 22-19-00783), work on manufacturing, work on manufacturing, study and application of amorphous-crystalline ribbons made of alloy $\text{Ti}_{50}\text{Ni}_{25}\text{Cu}_{25}$ were financially supported by grant from the Russian Science Foundation (project № 23-29-00779).

Compliance with ethical standards

All applicable international, national, and/or institutional guidelines for animal care and management were observed. This paper does not contain any studies with involvement of human beings as a subject of studies.

Conflict of interest

The authors declare that they have no conflict of interest.

References

- [1] M. Dijkstra, J.J. Van Baar, R.J. Wiegink, T.S. Lammerink, J.H. De Boer, G.J. Krijnen. *J. Micromech. Microeng.*, **15** (7), S132 (2005). DOI: 10.1088/0960-1317/15/7/019
- [2] S.N. Gorb. *Insect-Inspired Technologies: Insects as a Source for Biomimetics*. (In: A. Vilcinskis (eds) *Insect Biotechnology. Biologically-Inspired Systems*, Springer, Dordrecht, 2011). DOI: 10.1007/978-90-481-9641-8_13
- [3] H. Altner, H. Sass, I. Altner. *Cell Tissue Res.*, **176** (3), 389 (1977). DOI: 10.1007/BF00221796
- [4] D. Klocke, A. Schmitz, H. Soltner, H. Bousack, H. Schmitz. *Beilstein J. Nanotechnol.*, **2** (1), 186 (2011). DOI: 10.3762/bjnano.2.22
- [5] T.V. Kuznetsova, I.Yu. Severina. *ZhEBF*, **45** (4), 425 (2009). (in Russian)
- [6] J.C. Tuthill, R.I. Wilson. *Curr. Biol.*, **26** (20), R1022 (2016). DOI: 10.1016/j.cub.2016.06.070
- [7] A.A. Polilov. *PLoS ONE*, **12** (5), e0175566 (2017). DOI: 10.1371/journal.pone.0175566
- [8] D. Shaller. *Cell Tissue Res.*, **191** (1), 121 (1978). DOI: 10.1007/BF00223221
- [9] A.M. Lunichkin, M.I. Zhukovskaya. *ZhEBF*, **57** (1), 44 (2020). (in Russian) DOI: 10.31857/S004445292101006X
- [10] F. Marion-Poll, T.R. Tobin. *J. Neurosci. Methods*, **37** (1), 1 (1991). DOI: 10.1016/0165-0270(91)90015-R
- [11] M.A. Landolfi, J.P. Miller. *J. Comp. Physiol. A*, **177** (6), 749 (1995). DOI: 10.1007/BF00187633
- [12] A.M. Lunichkin, A.N. Knyazev. *ZhEBF*, **53** (6), 425 (2017). (in Russian)
- [13] K. Joshi, A. Mian, J. Miller. *J. Biomech. Eng.*, **138** (8), 081006 (2016). DOI: 10.1115/1.4033915

- [14] C. Magal, O. Dangles, P. Caparroy, J. Casas. *J. Theor. Biol.*, **241** (3), 459 (2006). DOI: 10.1016/j.jtbi.2005.12.009
- [15] M. Kanou, T Shimozawa. *J. Comp. Physiol. A*, **154** (3), 357 (1984). DOI: 10.1007/BF00605235
- [16] K.A. Slinker, C. Kondash, B.T. Dickinson, J.W. Baur. *Adv. Mater. Technol.*, **1** (9), 1600176 (2016). DOI: 10.1002/admt.201600176
- [17] F. Marion-Poll. *Entomol. Exp. Appl.*, **80** (1), 116 (1996). DOI: 10.1111/j.1570-7458.1996.tb00900.x
- [18] S. von Gratowski, V. Koledov, V. Shavrov, S. Petrenko, A. Irzhak, A. Shelyakov, R. Jede. *Advanced System for Nanofabrication and Nanomanipulation Based on Shape Memory Alloy* (In: *Frontiers in Materials Processing, Applications, Research and Technology*, Springer, Singapore, 2018)
- [19] V. Koledov, V. Shavrov, S. Von Gratowski, S. Petrenko, A. Irzhak, A. Shelyakov. *Conference Proceedings International Conference on Manipulation, Manufacturing and Measurement on the Nanoscale, 3M-NANO* (Taipei, Taiwan, 2014), 70573474. DOI: 10.1109/3M-NANO.2014.7057347
- [20] A. Shelyakov, N. Sitnikov, K. Borodako, V. Koledov, I. Khabibullina, S. von Gratowski. *J. Micro-Bio Robot.*, **16** (1), 43 (2020). DOI: 10.1007/s12213-020-00126-3
- [21] A.V. Shelyakov, N.N. Sitnikov, A.P. Menushenkov, R.N. Rizakhanov, A.A. Ashmarin. *Bull. Russ. Acad. Sci. Phys.*, **79** (9) 1134 (2015). DOI: 10.3103/S106287381509018X
- [22] A. Kamantsev, A. Mashirov, P. Mazaev, V. Koledov, V. Shavrov, V. Dikan, A. Shelyakov. *Microsc. Microanal.*, **21** (S3), 1999 (2015). DOI: 10.1017/S1431927615010776
- [23] G.I. Rozhkova. *Nejrofoziologiya tserkal'noj sistemy nasekomykh* (Nauka, M., 1993) (in Russian)
- [24] R. Heußlein, H. Gras, W. Gnatzy. *Functional Coupling of Cercal Filiform Hairs and Campaniform Sensilla in Crickets* (In: S.N. Gorb (eds) *Functional Surfaces in Biology*, Springer, Dordrecht, 2009), DOI: 10.1007/978-1-4020-6697-9_12
- [25] P. Schlossmacher, N. Boucharat, H. Rösner, G. Wilde, A.V. Shelyakov. *J. De Physique, IV: JP*, **112**(II), 731 (2003). DOI: 10.1051/jp4:2003986
- [26] A. Shelyakov, N. Sitnikov, S. Saakyan, A. Menushenkov, R. Rizakhanov, A. Korneev. *Mater. Sci. Forum*, **738–739**, 352 (2013). DOI: 10.4028/www.scientific.net/MSF.738-739.352

Translated by I.Mazurov